AIP | Applied Physics Letters

Determination of the deep donor-like interface state density distribution in metal/Al2O3/n-GaN structures from the photocapacitance–light intensity measurement

M. Matys, B. Adamowicz, and T. Hashizume

Citation: Appl. Phys. Lett. **101**, 231608 (2012); doi: 10.1063/1.4769815
View online: http://dx.doi.org/10.1063/1.4769815
View Table of Contents: http://apl.aip.org/resource/1/APPLAB/v101/i23
Published by the American Institute of Physics.

Related Articles

Nitrogen-passivated dielectric/InGaAs interfaces with sub-nm equivalent oxide thickness and low interface trap densities
Appl. Phys. Lett. 102, 022907 (2013)

Charge transport in HfO2 due to multiphonon traps ionization mechanism in SiO2/HfO2 stacks
J. Appl. Phys. 113, 024109 (2013)

A unique photoemission method to measure semiconductor heterojunction band offsets
Appl. Phys. Lett. 102, 012101 (2013)

Charge carrier relaxation and effective masses in silicon probed by terahertz spectroscopy
J. Appl. Phys. 112, 123704 (2012)

Digging up bulk band dispersion buried under a passivation layer
Appl. Phys. Lett. 101, 242103 (2012)

Additional information on Appl. Phys. Lett.

Journal Homepage: http://apl.aip.org/
Journal Information: http://apl.aip.org/about/about_the_journal
Top downloads: http://apl.aip.org/features/most_downloaded
Information for Authors: http://apl.aip.org/authors

ADVERTISEMENT

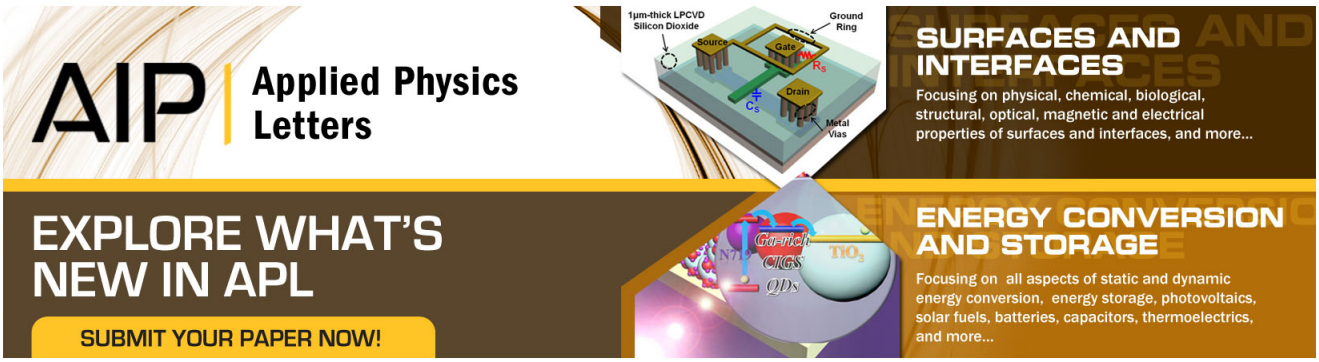

Determination of the deep donor-like interface state density distribution in metal/Al_2O_3/n-GaN structures from the photocapacitance–light intensity measurement

M. Matys,[1] B. Adamowicz,[1] and T. Hashizume[2]
[1]*Institute of Physics—Center for Science and Education, Silesian University of Technology, Krzywoustego 2, 44-100 Gliwice, Poland*
[2]*Research Center for Integrated Quantum Electronics, Hokkaido University, Kita-13 Nishi-8, Kita-ku, 060-8628 Sapporo, Japan*

(Received 22 May 2012; accepted 19 November 2012; published online 6 December 2012)

We developed a method for determining of the deep donor-like interface state density distribution $D_{it}(E)$ at the insulator/wide bandgap semiconductor interface in metal/insulator/semiconductor structures from the measurements of photocapacitance vs. ultraviolet light intensity $C_L(\Phi)$. From the comparison of theoretical and experimental $C_L(\Phi)$ curves we obtained the continuous donor $D_{it}(E)$ in the energy range between 0.15 eV and 1 eV from the valence band top for a metal/Al_2O_3/n-GaN device. In addition, the acceptor-like interface state $D_{it}(E)$ in the upper part of the bandgap was determined from the capacitance-voltage method. © *2012 American Institute of Physics*. [http://dx.doi.org/10.1063/1.4769815]

A metal/insulator/semiconductor (MIS) capacitor is a fundamental structure to study the insulator/semiconductor interface, especially to assess the energetic distribution of the interface states in the semiconductor bandgap, $D_{it}(E)$.[1] One of the methods for the determination of $D_{it}(E)$ is the Terman technique, in which the capacitance–voltage [$C(V)$] dependence measured at high frequency from the MIS diode is compared with the theoretical $C(V)$ curve calculated for the ideal device, i.e., without interface states.[2,3] This approach works very well for Si-based structures, however, in the case of wide bandgap semiconductors, e.g., GaN (bandgap of 3.4 eV at room temperature) and SiC (from 2.36 to 3.23 eV depending on polytype), very slow emission of carriers from the deep interface states to the conduction band (in n-type semiconductor) limits the energies for which $D_{it}(E)$ can be determined at room temperature to the interval approximately from $E_C - 1$ eV to E_C, where E_C is the conduction band minimum,[4,5] which is only about 1/3 of the bangap. In order to excite carriers from the deeper levels, higher temperature,[6–8] or light[9] can be applied. Using the former factor is limited by electrode thermal strength; thus, light seems to be more convenient for applications for device characterization. The photo-assisted capacitance measurement is sometimes used, but it is limited to the estimation of the total interface charge captured in the deep levels and released by the light[10–12] or average $D_{it}(E)$.[13]

In this letter, we developed a method for the determination of the interface state density distribution, $D_{it}(E)$, in the most part of the bandgap in n-GaN MIS structures. This approach is based on the combination of the Terman-like technique, which enables obtaining $D_{it}(E)$ in the upper part of the bandgap (step 1) from the high-frequency $C(V)$ characteristics, with the measurement of the photocapacitance versus light intensity $C_L(\Phi)$(step 2) supplying the information about the deep states in the bottom part of the bandgap. As a result of the measurement and analysis of two complementary dependencies $C(V)$ and $C_L(\Phi)$, the $D_{it}(E)$ spectrum in the large part of the bandgap can be obtained, in particular the deep donor states located near the valance band, which are extremely difficult to determine using standard electrical methods.

Our approach was applied in the determination of the continuous $D_{it}(E)$ spectrum for the metal/Al_2O_3/GaN structure. The device was fabricated using free standing n-GaN wafer (the doping level of 4×10^{16} cm^{-3}). The Al_2O_3 layer with a thickness of 23 nm was deposited by means of electron-cyclotron-resonance plasma-assisted process with an Al organic compound. The capacitance and photocapacitance were measured at 100 kHz by an impedance analyzer at room temperature. During the $C_L(\Phi)$ measurement, the gate bias of $V_G = -1.5$ V was applied and He-Cd laser light with a wavelength of 325 nm, and maximum power of 16 mW was used. The typical measured C_L transients after switch on and off the UV light are shown in Fig. 1. The steady-state condition was achieved after about 10 min. After switch off the light the photocapacitance is at first reduced relatively fast to a certain level which is then decreasing slowly. This latter effect is related to the long emission time of the carriers captured by the deep interface states. The applying of positive bias was necessary to obtain the initial state. We measured a very low leakage current of less than 3×10^{-8} A/cm^2 which is negligibly small for the C-V and photocapacitance

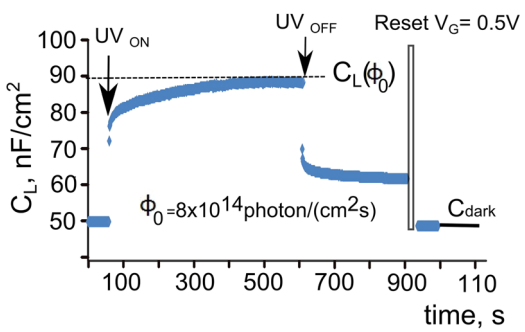

FIG. 1. Measured photocapacitance transients of metal/Al_2O_3/n-GaN structure after switch on and off the UV light at room temperature.

experiments. More details of structure fabrication technology can be found in Ref. 9.

The analysis of the experimental $C(V)$ and $C_L(\Phi)$ characteristics was based on the independence of the two applied measuring steps, which can be explained in terms of the dark Fermi level and photo-generated carrier densities or quasi-Fermi levels for electrons (E_{Fn}) and for holes (E_{Fp}) as shown in Fig. 2. In the case of the n-GaN-based device in the dark (step 1), the Fermi level scans the upper part of $D_{it}(E)$ upon the negative gate bias. Under illumination and negative gate potential (step 2), the photo-generated holes are attracted to the interface and their density depends highly on the light intensity, whereas the electrons are repelled from the interface. The excess holes can be captured by the donor interface states which charge positively whereas the acceptor states do not charge negatively due to the lack of electrons at the interface. Using the concept of the quasi-Fermi levels, one can say that E_{Fp} scans the bottom part of $D_{it}(E)$ during illumination due to increasing Φ whereas E_{Fn} is almost Φ-independent.

To calculate the capacitance and photocapacitance of the studied MIS structure, we used one-dimensional drift-diffusion model.[14] Under illumination by photons with energy above the bandgap, we assumed that each absorbed photon generates one electron-hole pair and the generation rate decreases exponentially with the distance from the interface according to the Beer-Lambert law. We took into account three main bulk recombination channels, i.e., band-to-band and Shockley-Read-Hall (SRH) recombination, and transitions through acceptor deep levels (related to so-called yellow luminescence), and also interface recombination through the continuous interface states distributed vs. energy according to the disorder induced gap state (DIGS) model[15] (Fig. 2)

$$D_{it}(E) = D_{it0}\exp\left(\left|\frac{E - E_{CNL}}{E_{0d,0a}}\right|^{n_{d,a}}\right), \tag{1}$$

where D_{it0} is the minimum density, E_{CNL} is the charge neutrality level ($E_{CNL} = E_C - 1.1$ eV in GaN) which is independent of insulator and interface treatment, E_{0d} (E_{0a}) and n_d (n_a) describe the shape of the donor (acceptor) branch of the interface states below (above) E_{CNL}, and they depend on insulator and interface processing. The DIGS states are attributed to a quasi-amorphous nature of the insulator/semiconductor interface.

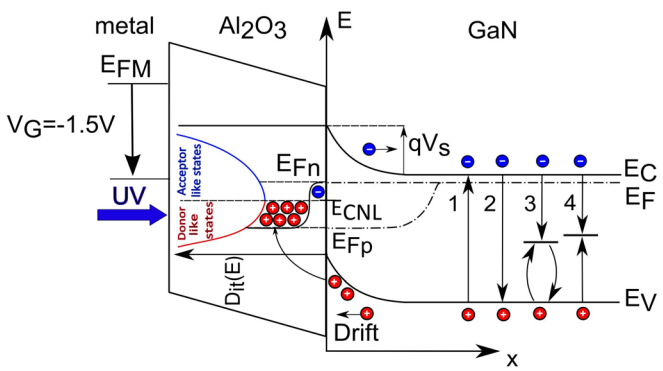

FIG. 2. The schematic presentation of the electronic phenomena analyzed in illuminated and negatively biased MIS structure, (1) electron-hole generation, (2) band to band recombination, (3) radiative point defect transitions, (4) non-radiative SRH recombination, V_s is the surface potential.

During the calculation of the charge in the interface states the following state occupation function was used

$$f_{it}(E) = \frac{\sigma_n n_s + \sigma_p p_1(E)}{\sigma_n[n_s + n_1(E)] + \sigma_p[p_s + p_1(E)]}, \tag{2}$$

where σ_n and σ_p are the interface state cross sections for capturing electron and holes, respectively, and n_s and p_s are the interface concentrations of electrons and holes, respectively. $n_1(E) = N_C\exp[(E - E_C)/(kT)]$ and $p_1(E) = N_V\exp[(E_V - E)/(kT)]$, where N_C and N_V are the effective densities of states in the conduction and valence band, respectively, k is the Boltzmann constant, and T is the temperature. In the dark, $f_{it}(E)$ is just the Fermi-Dirac distribution.

The charge in the DIGS states (Q_{it}) is described by the following formula:

$$\frac{Q_{it}}{q} = Q_{Dit} + Q_{Ait} = \int_{E_V}^{E_{CNL}} D_{it}\cdot(1 - f_{it})\,dE - \int_{E_{CNL}}^{E_C} D_{it}\cdot f_{it}\,dE, \tag{3}$$

where Q_{Dit} is the donor-like state charge and Q_{Ait} is the acceptor-like state charge. The interface electric field strength is given by

$$E_{it} = \frac{Q_{it}}{\epsilon_0\epsilon}, \tag{4}$$

where ϵ_0 is the vacuum permittivity and ϵ is the relative permittivity of GaN.

The interface recombination rate is given by the formula from SRH model generalized to the continuous energetic distribution of the traps

$$U_{it} = \int_{E_V}^{E_C} \frac{\sigma_n\sigma_p v_n v_p (n_s p_s - n_i^2) D_{it}(E)\,dE}{\sigma_n v_n[n_s + n_1(E)] + \sigma_p v_p[p_s + p_1(E)]}, \tag{5}$$

where v_n and v_p are the thermal velocities of electrons and of holes, respectively.

The boundary conditions are imposed by V_G, E_{it} and U_{it} at the insulator/GaN interface, and by zero potential at the Ohmic contact.

The model equations were solved self-consistently using the finite element method with a very good convergence (relative error at the level of 10^{-6}) to obtain the profiles of the carrier densities and of the electric potential in the MIS structure.

Finally, the capacitance and photocapacitance are calculated according to the following formula:

$$C = \frac{Q(V) - Q(V + \triangle V)}{\triangle V}, \tag{6}$$

where Q is the total charge in the whole structure and $\triangle V = 0.01$ V is the numerical equivalent of AC signal amplitude during $C(V)$ measurements. In the calculation of C and C_L, we assumed that the interface state charge cannot follow fast AC voltage signal but can follow the slow gate

voltage sweep (high-frequency measurement). We excluded the influence of the interface states below $E_C - 1\,\text{eV}$ on the dark $C(V)$ curve, but we took them into account during the calculation of $C_L(\Phi)$. It should be also mentioned that in n-GaN in the dark, the hole concentration can be excluded even under strong negative gate bias (deep depletion) due to an extremely low generation rate.[13]

Under illumination, the applied gate bias ($V_G = -1.5\,\text{V}$) assured the non-radiative interface recombination quenching, as shown in the inset in Fig. 3. The bell-like curves of U_{it} vs. V_G strongly decay upon negative bias from the maximum value (for $p_s = n_s$) due to electron repelling from the interface in spite of high $D_{it}(E)$ and large interface state cross sections for electron capturing (σ_n). Furthermore, the very low concentration of electrons (with respect to holes) in the depletion layer causes that the $f_{it}(E)$ function, and thus Q_{it} under UV excitation, is practically independent of σ_n and σ_p (Eq. (2)). It is also evident from Fig. 3 that the interface hole concentration (p_s) and thus the quasi-Fermi level position (E_{Fp}) is mainly determined by $D_{it}(E)$ and not by the bulk SRH lifetime τ. The latter parameter modifies $p(x)$ only in the bulk. It also should be noted that in the calculations we excluded both the leakage current because of the high quality passivation of the investigated MIS structures, and interface fixed charge, which was excluded from C-V analysis. All these properties of MIS-GaN under UV-excitation provide the basis for the quantitative assessment of the deep donor interface states from the analysis of C_L vs. Φ characteristics.

Fig. 4 presents the dark $C(V)$ curves calculated for different $D_{it}(E)$ distributions, including the flat one as shown in the inset. The best fitting of theoretical dependencies to the experimental data is obtained for $D_{it0} \approx 10^{11}\,\text{eV}^{-1}\,\text{cm}^{-2}$ (curve 1) which is in agreement with the results for the similar structures[16–18] obtained from the Terman technique and photo-assisted C–V technique. It should be pointed out that only $D_{it}(E)$ in the upper part of the bandgap (approximately between E_{CNL} and E_C) is determined at room temperature so the $C(V)$ curve is insensitive to the bottom part of $D_{it}(E)$.

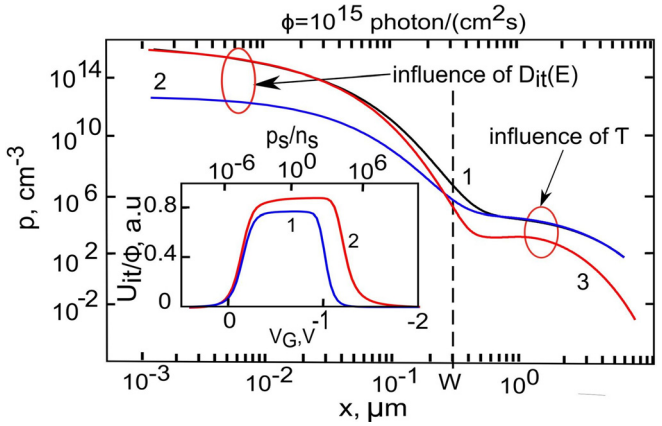

FIG. 3. Calculated in-depth profiles of hole concentration $p(x)$ in GaN, where x is the distance from the surface, for different interface state density and bulk lifetime: $D_{it0} = 10^{11}\,\text{eV}^{-1}\,\text{cm}^{-2}$ and $\tau = 10^{-7}s$ (curve 1), $D_{it0} = 2 \times 10^{11}\,\text{eV}^{-1}\,\text{cm}^{-2}$ and $\tau = 10^{-7}\,\text{s}$ (2), and $D_{it0} = 10^{11}\,\text{eV}^{-1}\,\text{cm}^{-2}$ and $\tau = 10^{-9}$ s (3). Inset: interface recombination rate U_{it} per one incident photon for different interface state cross section for electron capturing $\sigma_n = 10^{-15}\,\text{cm}^2$ (curve 1) and $\sigma_n = 10^{-14}\,\text{cm}^2$ (2) $\tau = 10^{-7}\,\text{s}$, $D_{it0} = 10^{12}\,\text{eV}^{-1}\,\text{cm}^{-2}$. W is the depletion layer width.

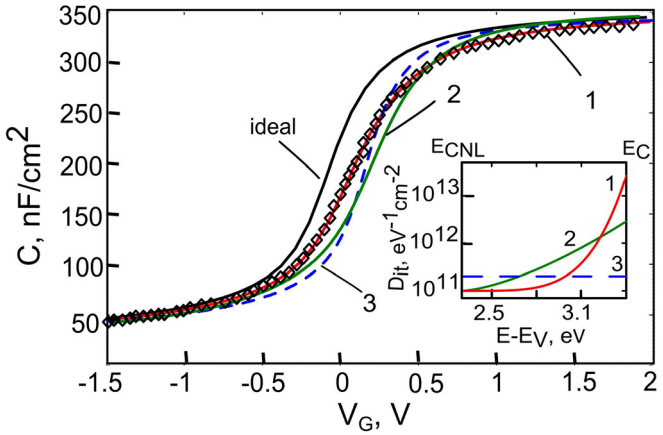

FIG. 4. Calculated capacitance-voltage characteristics for the ideal MIS structure (without interface states) and for various interface state density distributions as shown in the inset.

The second step of our method is presented in Fig. 5 which shows the measured $C_L(\Phi)$ curve (points) compared with the calculated ones for various $D_{it}(E)$ (in the inset) in the bottom part of the GaN bandgap (approximately between E_V and E_{CNL})). It should be noted that $D_{it}(E)$ functions with different curvatures were chosen to result in the simulated $C_L(\Phi)$ curves close to the experimental data. For comparison, $C_L(\Phi)$ dependencies for ideal and very good (curve 4) interfaces were calculated to prove the high sensitivity of our method to low $D_{it}(E)$ values. In addition, E_{Fp} variations in the bandgap were simulated (curve 5, $D_{it}(E)$ of curve 2) to show the energy range scanned during illumination in our experiment (between about 1 eV and 0.15 eV from the valence band top at the interface, E_{Vs}). The corresponding relationship between E_{Fp} and $C_L(\Phi)$ is presented in the inset in Fig. 6. From Fig. 5 it follows that the changes of C_L vs. Φ are governed mainly by donor $D_{it}(E)$ in terms of the positive interface charge Q_{Dit} (Eq. (3)) variations upon excitation. In the Φ range up to the point A, the $C_L(\Phi)$ signal is related to the interface potential V_s decrease (with respect to the dark band bending) caused by charging the donor states due to capturing photo-holes. One can note that the larger $C_L(\Phi)$

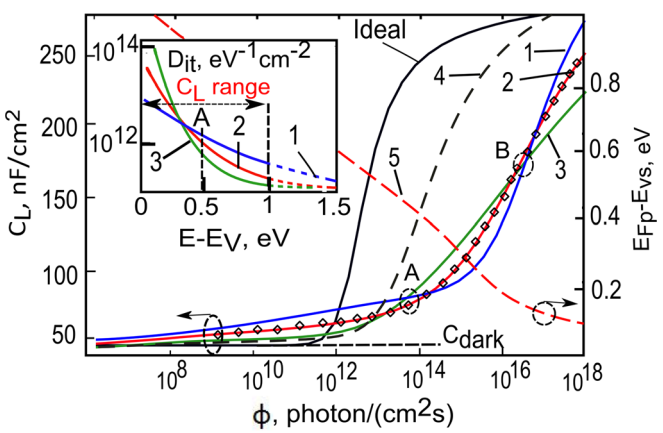

FIG. 5. Calculated photocapacitance-light intensity curves (1–3) for various interface state density distributions as shown in the inset. Curve 4 corresponds to $D_{it0} = 5 \times 10^{10}\,\text{eV}^{-1}\,\text{cm}^{-2}$ and shape of curve 1. Ideal curve is for $D_{it0} = 0$. Curve 5 represents E_{Fp} position with respect of the valence band top at the surface (E_{vs}) vs. Φ for $D_{it}(E)$ of curve 2. The points represent the experimental data.

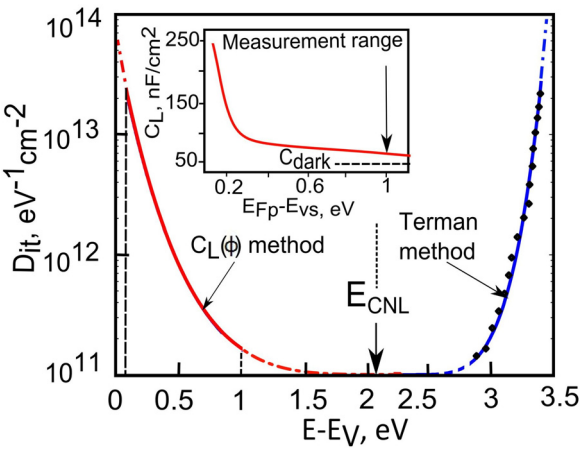

FIG. 6. The interface state density distribution $D_{it}(E)$ determined by using the presented method (solid lines) and the part derived from Terman technique (points). The dashed line means the approximated parts of $D_{it}(E)$ with exponential function. Inset: relationship between C_L and E_{Fp} position at the interface.

(curve 1 with respect to 3) corresponds to higher Q_{Dit} which changes V_s stronger than lower donor charge. On the contrary, in the range of stronger excitations above the point A, one can observe the opposite relationship among $C_L(\Phi)$ curves because in this case $C_L(\Phi)$ is mainly determined by free excess holes collected near the interface in GaN. Therefore, $C_L(\Phi)$ is larger for lower Q_{Dit} (curve 3 with respect to 1 below the point B and curve 1 with respect to 3 above point B) since the holes captured by the donor states do not contribute to $C_L(\Phi)$. The cross section point B corresponds to the situation when Q_{Dit} reaches the same value for all assumed $D_{it}(E)$.

In Fig. 6, we displayed the $D_{it}(E)$ obtained in the large energy range both from the $C_L(\Phi)$ (about 1/3 of the bandgap) and C(V) (about 1/3) methods. It exhibits typical for the DIGS model almost symmetric U-like shape with the approximated minimum D_{it0} of about $10^{11}\,\mathrm{eV}^{-1}\,\mathrm{cm}^{-2}$. The determined distribution is in good agreement with the fragmentary data derived using the classical Terman technique. It should be enhanced that an important advantage of the $C_L(\Phi)$ method is its independence of bulk non-equilibrium effects. Furthermore, the described method can be used in the case of narrower bandgap semiconductors (using visible light instead of UV) at lower measurement temperatures. It is also worth mentioning that an alternative technique to the $C_L(\Phi)$ method is to investigate MIS structures using C-V technique in structures grown on both p- and n-type semiconductor.

In conclusion, we developed a method based on the analysis of photocapacitance versus UV excitation intensity for quantitative assessment of the donor-like interface state density $D_{it}(E)$ in a wide energy range, which was successfully applied to the metal/Al_2O_3/n − GaN structure. We believe that the proposed approach will be very useful for characterisation of other wide bandgap material interfaces in cases where the standard electric methods fail.

The authors are grateful to the late Dr. Marcin Miczek for his contribution to the paper elaboration and valuable discussions.

The work was partially supported within InTechFun project (UDA-POIG.01.03.01.00-159/08-04) of European Union Structural Funds in Poland.

[1]E. H. Nicollian and J. R. Brews, *MOS (Metal Oxide Semiconductor) Physics and Technology* (Wiley, New York, 1982).
[2]L. M. Terman, Solid-State Electron. **5**, 285 (1962).
[3]R. Engel-Herbert, Y. Hwang, and S. Stemmer, J. Appl. Phys. **108**, 124101 (2010).
[4]J. A. Cooper, Phys. Status Solidi A **162**, 305 (1997).
[5]M. Miczek, C. Mizue, T. Hashizume, and B. Adamowicz, J. Appl. Phys. **103**, 104510 (2008).
[6]M. Miczek, B. Adamowicz, C. Mizue, and T. Hashizume, Jpn. J. Appl. Phys. **48**, 04C092 (2009).
[7]K. Ooyama, H. Kato, M. Miczek, and T. Hashizume, Jpn. J. Appl. Phys. **47**, 5426 (2008).
[8]B. Gaffey, L. J. Guido, X. W. Wang, and T. P. Ma, IEEE Trans. Electron Devices **48**, 458 (2001).
[9]C. Mizue, M. Miczek, J. Kotani, and T. Hashizume, Jpn. J. Appl. Phys. **48**, 020201 (2009).
[10]J. Tan, M. K. Das, J. A. Cooper, and M. R. Melloch, Appl. Phys. Lett. **70**, 2280 (1997).
[11]T. Marron, S. Takashima, Z. Li, and T. P. Chow, Phys. Status Solidi C **9**, 907 (2012).
[12]B. L. Swenson and U. K. Mishra, J. Appl. Phys. **106**, 064902 (2009).
[13]T. Hashizume, E. Alekseev, D. Pavlidis, K. S. Boutros, and J. Redwing, J. Appl. Phys. **88**, 1983 (2000).
[14]S. Selberherr, *Analysis and Simulation of Semiconductor Devices* (Springer, Wien, 1984).
[15]H. Hasegawa and H. Ohno, J. Vac. Sci. Technol. B **4**, 1130 (1986).
[16]Y. Hori, C. Mizue, and T. Hashizume, Jpn. J. Appl. Phys. **49**, 080201 (2010).
[17]Y. Q. Wu, T. Shen, P. D. Ye, and G. D. Wilk, Appl. Phys. Lett. **90**, 143504 (2007).
[18]Y. Hori, C. Mizue, and T. Hashizume, Phys. Status Solidi C **9**, 1356 (2012).